Influence of dewetting on the damping properties of a filled polymer system: 2. Damping properties

Y. Diamant and M. Folman
Department of Chemistry, Technion, Israel Institute of Technology, Haifa, Israel
(Received 16 August 1979)

Following characterization of the processes observed by adding an inert filler into an elastomer, hysteresis and wave-propagation meaurements were carried out which indicate that dewetting is the main factor that causes an increase in the damping, and is responsible for the softening effect observed in PBCT filled with spherical Al powder. Other factors, such as stress concentration, friction between unbonded filler particles and rearrangement of the dewetted chain molecule configuration, have only a secondary effect on damping. The results showed an increase in damping with higher volume fraction of filler and greater particle size. The softening energies, calculated from successive hysteresis, are in agreement with the apparent activation energy difference obtained from shifting stress-strain data to a reference temperature and reference filler volume fraction. Definition of a loss function-tan Λ from the hysteresis data contributes to the understanding of the mechanisms that play a role in the increasing damping of the composite, and in the influence of dewetting on the observed transition. Wave propagation experiments gave similar results.

INTRODUCTION

The viscoelastic behaviour of polymers is responsible for their damping properties. Quantitatively, damping will depend on the materials and on the conditions (such as temperature and/or frequency) under which the deformation is applied.

The addition of a filler to an elastomer influences its mechanical as well as its damping properties. Theoretical efforts were made to describe the behaviour of composites as a function of the filler and binder properties[1–4]. According to these theories[2–4], an addition of a stiff elastic filler reduces the viscoelastic fraction of the material thereby reducing damping. On the other hand the new processes introduced into the system by the addition of the filler may increase the damping, as has been observed in several systems[5–7].

In an adhered filler elastomer under tension, dewetting occurred. This process may be divided into two steps: (1) debonding of filler particle from the binder; (2) the rearrangement of the torn chain molecules in the new equilibrium state. Both steps absorb energy, the first owing to the creation of new surfaces and the second because of the energy required to overcome the potential barriers of the molecule configurations and the movement of the chains in a viscous medium.

In the present study efforts were made to investigate the role these processes play in the damping increase observed in composites, which is important as more plastic materials are used in energy damping systems, for example, shock absorption, vibration damping, acoustic insulation etc.

No attempt was made to deal with thermomechanical coupling and multiple scattering effects which contribute to high damping when the particle size of the filler is of the same order as the wavelength, in the case of wave propagation[8]. Both effects can be neglected, the first because no heating of the specimens was observed, and the second because the wavelength was much longer than the size of the filler.

BACKGROUND

Hysteresis

A general explanation of the hysteresis phenomena has been given by domain theory[9]. Assuming that no chemical bonds are broken, the hysteresis phenomena observed in polymers are mainly due to the viscoelastic behaviour of the materials and therefore higher hysteresis losses are obtained in the glass-transition region. Addition of a filler may increase the hysteresis compared to that of the pure binder. The major mechanism responsible for this increase depends on the system investigated. In carbon black vulcanizate rubber, the effect of 'multiple strain' was found to be responsible for the higher hysteresis obtained at high strain level, while the breakdown of carbon black aggregates explains the higher hysteresis at low strains[10]. In other vulcanizates this explanation does not hold, as the store-and-loss moduli were found to be independent on the strain amplitude[11]. In an unreinforced filled elastomer, the interface interaction will have a major effect on the hysteresis.

A further phenomenon, observed in filled polymers, is the well known Mullin's effect which results in softening of the material when repeated stress-strain cycles are applied on a composite, with the maximum stress or strain in the first cycle not exceeded. Several explanations were given for this effect in vulcanized rubbers[12,13]. In an unreinforced filled elastomer, it was found that dewetting is responsible, as no softening was observed at high strains after dewetting was completed[14]. Determination of SBR filled with various particle size polystyrene and poly(methyl methacrylate)[15], indicate that the hysteresis losses in the first and the third cycle were linear with the mechanical energy applied to deform the materials. While in the first cycle the data for all materials investigated fall on one line, a split was observed in the third cycle. The slopes of the lines were taken as a measure of dewetting; it was shown that the use of larger particles resulted in higher hysteresis losses.

0032-3861/80/091079-08$02.00

Wave propogation

By neglecting radial inertia and assuming that the specimen cross-section remains planar and the stress is uniformly distributed over the cross-section, the displacement, U, of a wave, propagating in a long viscoleastic rod in the x direction (uniaxial stress) is given by:

$$U_{x,tt} = \frac{E^*}{\rho} U_{x,xx}$$

where ρ is the density of the rod and E^* is the complex Young's modulus:

$$E^* = E_1 + iE_2 \tag{2}$$

The solution of the above equation is:

$$U(x,t) = U_0 \exp(-\alpha x)\exp[i\omega(t - x/c)] \tag{3}$$

where ω is the frequency of the wave, α its attenuation and c the wave velocity:

$$c = \frac{|E^*|}{\rho} \tag{4}$$

Substitution of equations (2), (3) into the wave equation (1) and separation of the real and imaginary parts results in:

$$\frac{E_1}{\rho} = \frac{1 - \left(\frac{\alpha c}{\omega}\right)^2}{\left[1 + \left(\frac{\alpha c}{\omega}\right)^2\right]^2} \tag{5}$$

$$\frac{E_2}{\rho} = \frac{2\left(\frac{\alpha c}{\omega}\right)c^2}{\left[1 + \left(\frac{\alpha c}{\omega}\right)^2\right]^2}$$

It can be seen from equation (5) that by determination of the attenuation and the velocity of the wave, the real and imaginary parts of the complex modulus can be evaluated.

On the assumption that the rod is very long and/or the attenuation is very high, so that reflection from the far end of the rod can be neglected and the location of the pick-up along the rod does not influence the wave[16,17], the ratio of the displacement at the point ($x = 0$) (wave entrance) to that at the measuring point ($x = m$), if described by the imaginary part of equation (3), is given by:

$$\frac{U_{x=0}}{U_{x=m}} = \frac{A \sin(\omega t + \beta)}{B \sin \omega t} \tag{6}$$

where β is the phase difference of the wave between the two points:

$$\tan\beta = \frac{1 + M\exp(-2\alpha m)}{1 - M\exp(-2\alpha m)} \tan km \tag{7}$$

and $(A/B)^2$ the square of the displacement amplitude at these points:

$$\left(\frac{A}{B}\right)^2 = \frac{1 - M\exp(-2\alpha m)\cos 2km + M^2\exp(-\alpha m)}{(1 - M)^2\exp(-2\alpha m)} \tag{8}$$

where M is a constant describing the reflection of the wave by the pick-up and k is given:

$$k = \frac{\omega}{c} \tag{9}$$

If the attenuation is high, equation (10) gives $\ln B$ as:

$$\ln B = \alpha m + \ln A - \ln(1 - M) = -\alpha m + \ln C \tag{10}$$

so that a plot of the amplitude B as a function of the distance x on a semilog scale will result in a straight line, the slope of which will give the wave attenuation α. The phase can be derived in this case from equation (7):

$$\beta = km \tag{11}$$

By using equation (9), the wave velocity c can be evaluated.

EXPERIMENTAL

The materials used, their preparation, and the specimen used for the hysteresis experiment, have been described elsewhere[18]. For wave propagation 4 x 10 x 1 000 mm specimens, were prepared by moulding.

Hysteresis

Repeated hysteresis experiments were carried out on an Instron apparatus at −60°, −50°, −40°, −25°, 0°, +25°C, and at a constant crosshead speed of 10 cm min^{-1}. The specimens were deformed to a maximum strain and then released to their initial length for 4–5 successive times. Between the straining cycles, the specimens were allowed to relax free from stresses at the experiment temperature for half the cycle period. This period was defined as being twice the time to strain and release the specimen (to maximum strain). After a few minutes, required for stabilizing the Instron cabinet temperature, the specimen was strained again. It was found that after this relaxation procedure, the specimens returned to their initial length to within 1.5%. The experiments were repeated in 4–5 different maximum strain levels in the range of 0–100%. The hysteresis losses H were calculated from the differences in the area under the stress-strain curve on straining W_1 and releasing W_2:

$$H = W_1 - W_2 \tag{12}$$

Wave propagation

Wave propagation experiments were conducted at temperatures of −25°C, 0°C and 25°C, in the frequency range 100–7000 Hz, where the wave was also superimposed on static strains. The experimental set-up is described in *Figure 1*. The source of the wave was a Ling–Altec Shacker (Model 408). The frequency was determined by an Exact Electronics oscillator (Model 504). Wave propagation through the rod was detected by a crystal monophonic pick-up (Ronette model DC-289), installed on a holder that could be

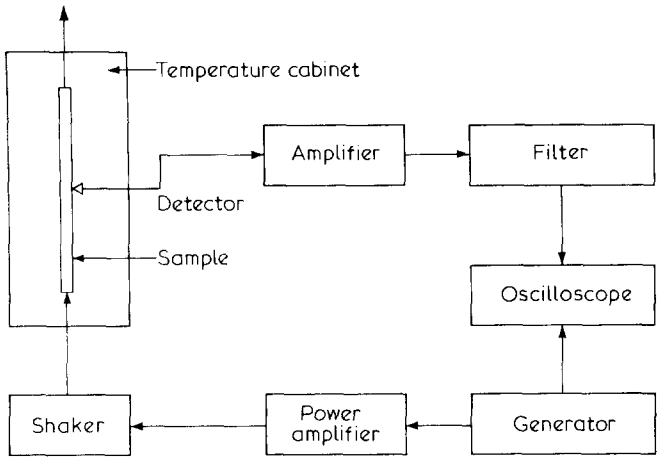

Figure 1 Block diagram of the wave propagation experimental set-up

moved along the specimen manually by use of a screw from outside the temperature cabinet. The holder also insured that the cartridge applied a constant force of 4 g to the specimen. The output of the pick-up was amplified and filtered and then recorded on the y axis of an oscilloscope. For measuring the wave velocity, the oscillator output was directly fed to the x axis, so that half of the wavelength $\lambda/2$ was evaluated from the distance between two successive degenerating points of the Lissajou curve. Knowing the frequency, the wave velocity could be calculated from:

$$c = \omega\lambda \qquad (13)$$

The specimen was connected rigidly to the shaker on one side, and to a nylon string on the other side. By pulling the string (through a pulley), the specimen was strained to a constant static strain. Three thermocouples along the specimen were used to measure the temperature. After a uniform temperature in the cabinet was reached, a wave of constant frequency was generated through the specimen. The velocity of the wave was determined as described previously. By moving the pick-up along the rod and recording on the oscilloscope the wave amplitude as a function of the distance from the wave entering point, the attenuation of the wave could be calculated. Using equation (5), the real and imaginary parts of the complex modulus could be evaluated.

The restrictions of the experimental technique result from the properties and the dimensions of the specimens. At low frequencies ($\omega < 100$ Hz), the wave length is almost equal to the length of the specimen, which reduces the accuracy of the measured velocity. The attenuation in this range is small, which leads to an error in its determination, as the reflection of the wave from the far end of the rod cannot be neglected. Calculations showed that if a reflection of less than 10% of the incident wave is required, the attenuation should be 0.030 mm^{-1}. At high frequencies ($\omega > 5000$ Hz), the wavelength is almost of the same order as the lateral dimensions of the specimen. Therefore interference with lateral waves may occur, and the assumptions on which the derivation of the wave equation is based no longer hold. In this range, the attenuation is very high and the wave decays too fast, so that errors are introduced in the determination of the wave velocity and attenuation. To overcome these restrictions, thinner and longer specimens should be used. The high viscosity of the material before moulding, and the required dimensions of the experimental set up, meant that such specimens were not used, and therefore only a narrow range of frequencies was determined.

RESULTS AND DISCUSSION

Hysteresis

The results obtained on repeating hysteresis experiments are illustrated schematically in *Figure 2*. The first hysteresis loop is described by curves (1) and (2). As long as the maximum stress or strain of the first cycle is not exceeded (point A), a 'softening effect' is observed. It was found that the descending curves obtained on releasing the stress of the successive cycles are almost overlapping and only the straining curves are changing. This is shown in *Figure 2* by curves (1,3) and (2,4). After 3–4 cycles, the hysteresis losses remained constant and no further changes were observed.

Differences in the hysteresis between the first and the fourth cycle (after the hysteresis losses become constant) can be related to irreversible processes, which occur during the straining, such as the breaking of chemical bonds. The hysteresis losses at the fourth cycle are primarily related to the viscoelastic character of the material. It was found that 'softening' occurs mainly in the first cycle, while the hysteresis losses in the second and third cycles are close to the value obtained in the fourth cycle.

Figures 3,4 describe the hysteresis losses of the material in the 1st and 4th cycles as a function of the mechanical energy required to deform the material to the maximum strain. All the data points obtained in the temperature range −60 to +25°C, and with maximum strains 0–100%, can be described approximately by a straight line. This linearity indicates thermorheologically simple and linear viscoelastic properties.

The slopes of the lines, which express the hysteresis losses per unit strain energy input, were calculated by a least squares technique and are listed in *Table 1*. Almost the same slope was obtained in the 1st and 4th cycles for the pure polymer, while for the filled materials the difference in the slope between the 1st and 4th cycle increases with the volume fraction of the filler. This indicates that the observed softening effect is caused by processes that are introduced

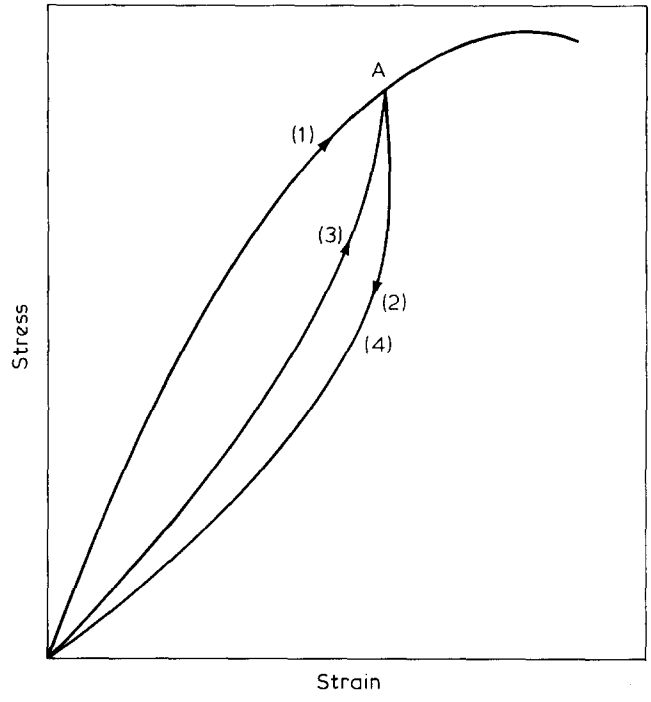

Figure 2 Typical successive hysteresis cycles

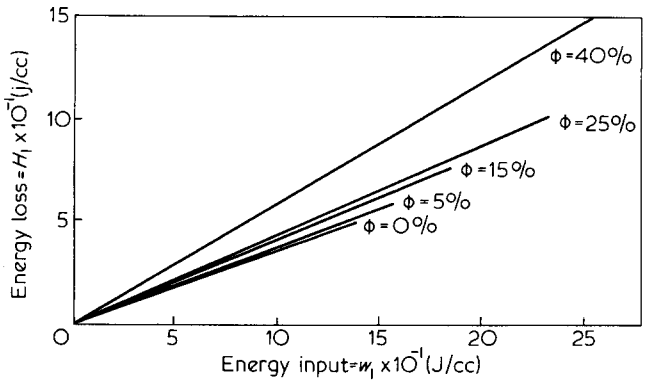

Figure 3 Hysteresis energy in the 1st cycle *versus* the input strain energy as a function of filler content

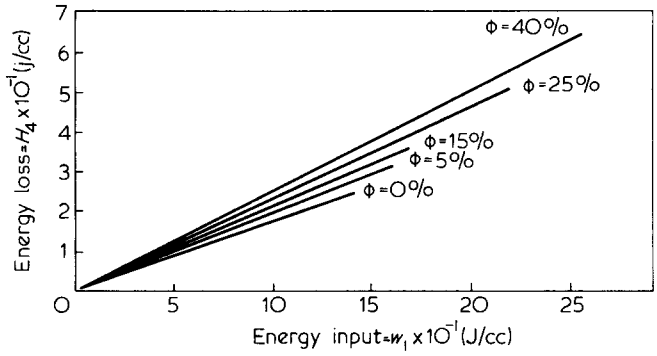

Figure 4 Hysteresis energy in the 4th cycle *versus* the input strain energy as a function of filler content

into the system by adding the filler, such as internal friction, dewetting and rearrangements of the torn molecule configurations, which depend on filler content.

If no irreversible processes, such as the breaking of chemical bonds, are involved, it is expected that as long as the maximum strain in the first cycle is not exceeded, the dewetting process is taking place only in the 1st cycle. Almost no rewetting of the debonded molecules is expected, as the specimens were subjected only to a short relaxation period between straining cycles. Therefore the difference of the hysteresis losses between the 1st and 4th cycles are due to dewetting. The small differences of the hysteresis losses in the 4th cycle between different materials are attributed to the above processes, excluding dewetting. Data in *Table 1* support expectations. The difference of the hysteresis losses between the 1st and 4th cycle, namely the softening effect ΔH, can be taken as a measure of the dewetting energy:

$$\frac{\Delta H}{W_1} = \frac{H_1 - H_4}{W_1} \tag{14}$$

where H_1 and H_4 are the hysteresis energy losses in the 1st and the 4th cycle respectively, and W_1 is the energy required to deform the specimen to the maximum in the 1st cycle.

The conclusion can be drawn that the softening effect can be attributed to dewetting is correct as long as no breaking of chemical bonds occurs, because in this case the softening will be mainly due to this process.

Confirmation of the assumption that no chemical bonds were broken during deformation is obtained from the following observed results:

(1) swelling results[18];
(2) a linear relation between hysteresis energy losses and deforming energy;
(3) no softening was observed in the pure polymer, which indicates that all the irreversible processes are due to the addition of the filler;
(4) *Figure 5* describes the difference of hysteresis losses between the 1st and 4th cycles, plotted against the apparent energy obtained from the second shift factor log a_ϕ[18]; the linear relation also indicates that most of the softening is due to dewetting. The bonding energy between the filler and the binder W_a, is given approximately by the relation:

$$W_a = 2(\gamma_s \gamma_p)^{1/2} \tag{16}$$

where the surface energy of the polymer γ_p was taken from the result obtained in reference 18, 35 dyne cm^{-1} and the surface energy for Al (= γ_s) is 272 dyne cm^{-1} [19].

As the surface area, Al of the powder was found to be 0.75 m^2 gm^{-1} and the densities of the materials are given elsewhere, the bonding energy per unit volume could be calculated:

$$W_a = (0.145 - 0.245)\,\text{joule cm}^{-3}$$

This value is in agreement with the softening energies obtained. On the other hand, if breaking of chemical bonds is involved, the expected energy losses should be much higher. If the C–C bond energy is taken as 82 kcal/mol and the cross-link density is given approximately by:

$$\rho/Mc \cong 10^{-4}\ \text{mol cm}^{-3}$$

The energy per unit volume will be given by:

$$W = 35\ \text{joule cm}^{-3}$$

which is 200 times higher than the observed softening losses.

Table 1 Hysteresis energy in the 1st and 4th cycles in relation to energy input

Composition	ϕ	H_1/W_1	H_4/W_1	$\Delta H/W_1$
B-1	0	0.1858	0.1846	0.0012
B-2	5	0.2460	0.2186	0.0276
B-3	15	0.2925	0.2242	0.0683
B-4	25	0.4506	0.2446	0.2060
B-5	40	0.6373	0.2590	0.3783
B-6	25*	0.4966	0.2173	0.2793

* Particle size of 30μ

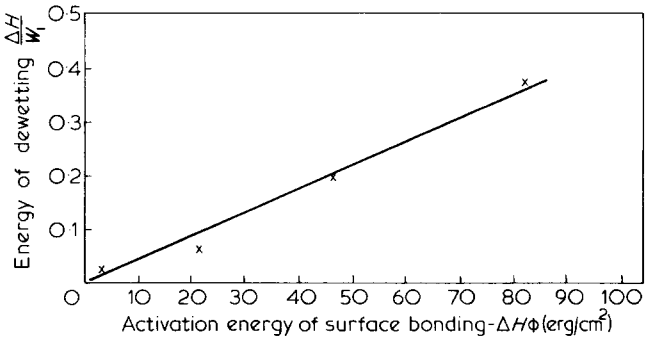

Figure 5 Dewetting energy *versus* the apparent activation energy of adhesion attachements

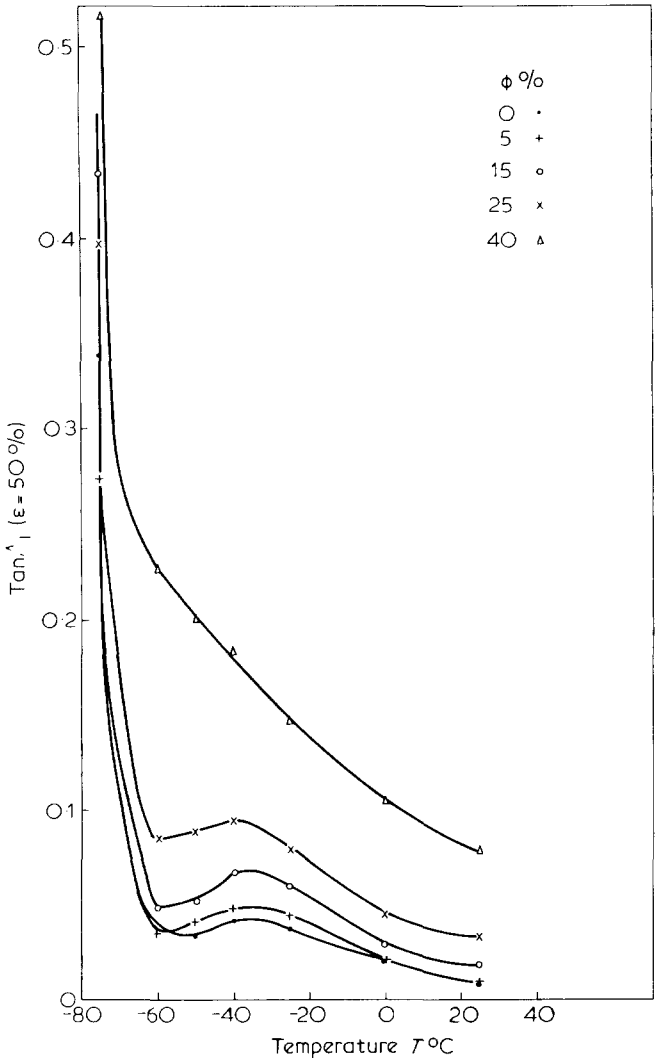

Figure 6 The loss function (tan Λ_1), obtained in the 1st cycle at 50% strain *versus* temperature, and as a function of filler content

Loss function

As in the hysteresis experiments, high deformations are applied on the material during only half a period (tension), this is not a sinusoidal form of deformation. For that reason the hysteresis energy H could not be related to the material property tan δ through:

$$\tan \delta = \frac{H}{2\pi W_2} \tag{16}$$

where tan δ is defined by:

$$\tan \delta = \frac{E_2}{E_1} \tag{17}$$

and W_2 is the reversible part of the mechanical work applied to deform the material.

Therefore, a loss function is defined:

$$\tan \Lambda = \frac{H}{2\pi W_2} \tag{16a}$$

It is clear from the experimental conditions that:

$$\tan \delta \neq \tan \Lambda$$

but qualitatively both functions are expected to behave in the same way, which means that if there is a shift to one direction in tan δ, a shift in the same direction in tan Λ will occur; or an increase in tan δ will result in an increase in tan Λ, although the magnitude of the shift, or of the increase, will not be the same.

Figure 6 - 7 describes tan Λ obtained from the hysteresis data as a function of temperature, at a maximum strain of 50% in the 1st and the 4th cycles. The figures indicate the existence of a transition above T_g. The intensity of the transition increases with the volume fraction of the filler, and at $\phi = 40\%$ it disappears, probably because of the high damping, but it appears in the 4th cycle as a shoulder. In the 1st cycle the maximum of this transition is higher and also the differences between the materials are more pronounced than in the 4th cycle, except for the pure polymer, where the difference between the 1st and 4th cycles is negligible.

Figures 8–9 describe tan Λ_1 and tan Λ_4 *versus* the temperature as a function of maximum strain. For the pure polymer, all the data points at strain levels between 0–100% fall almost on the same line (*Figure 8*). This shows simple thermorheology and linear viscoelastic behaviour. A split in the loss function tan Λ_1 and tan Λ_4 is observed for the filled materials. The secondary maximum of these functions becomes higher as the volume strain fraction of the

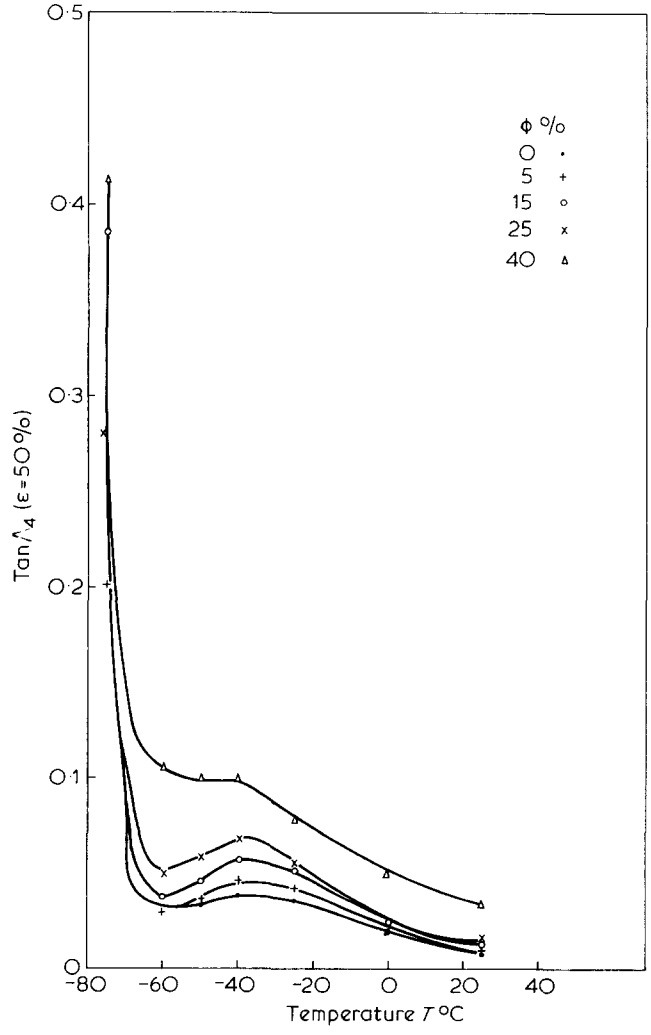

Figure 7 The loss function (tan Λ_4), obtained in the 4th cycle at 50% strain *versus* temperature, and as a function of filler content

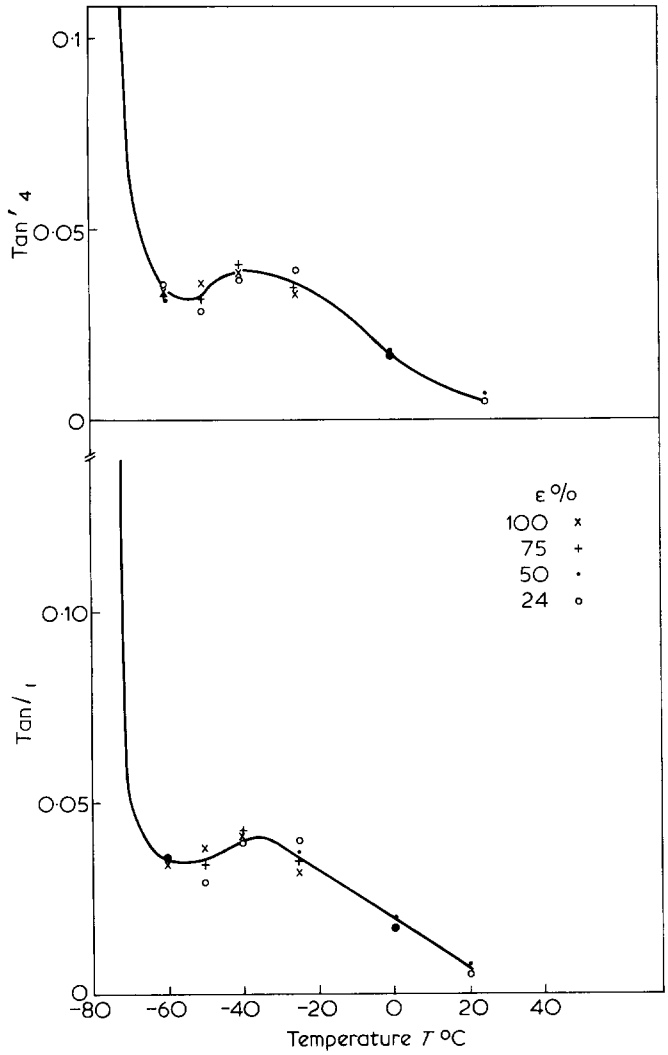

Figure 8 The loss function (tan Λ) obtained in the 1st and 4th cycle *versus* temperature and as a function of strain for B-1 composition (ϕ = 0%)

filler is increased, while at higher temperatures almost no difference could be observed. In addition, a shift of this secondary maximum toward lower temperatures was also observed. This shift increases with the strain level. Both these findings indicate that the transition is influenced by the dewetting process. Increasing the filler volume fraction ϕ will increase the interface surface area, i.e. the number of interface bonds and, therefore, the dewetting will depend on ϕ. On the other hand, increasing the strain level also increases the degree of dewetting. Therefore, higher strain and filler volume fraction will result in higher dewetting and thereby higher energy losses will be observed. On the assumption that this transition is governed by an energy barrier, the higher the mechanical energy supplied into the system, the lower will be the thermal energy needed. Therefore at higher strains, larger shifts to lower temperature of this transition are obtained (*Figure 9*). The same results were also obtained in the 4th cycle, but the difference was less pronounced; this was also true for the other materials. The dependence of the damping on the strain in the filled composite, indicates a non-linear viscoelastic behaviour in the transition zone that is in contrast to the results for the pure polymer. On the addition of a filler into the material, a new mechanism, dewetting, is introduced and this nonlinear behaviour results in the fact that at every level of straining a different material, characterized by a different dewetting level, is obtained. The small differences in the 4th cycle indicate that all other mechanisms like friction, rearrangement of configurations and dewetting of rewetted bonds, have only a minor effect on the energy losses.

As the secondary transition above T_g was also observed in the unfilled polymer (see *Figure 8* and other studies[20,21]). it could not be explained as a dewetting transition, as it was by Lepie and Adicoff[22]. They adopted a Beer–Lambert law to describe quantitatively this transition when a PBCT based propellant was investigated. Their findings and the results of this study, indicate that this transition is independent of the filler used and the explanation should be based on a transition existing in the polymer, but is effected by the addition of a filler and dewetting. Previous studies on polybutadiene[23] indicate the existence of a transition above T_g, when mixtures of high and low molecular weight polybutadiene were investigated. It was found that this transition is associated with the movement of the low molecular weight component as a whole and its intensity as the crosslink density increases and almost disappears at high crosslink density ($M_c \leqslant 4\,400$). But the low percentage of extract obtained[20] for PBCT indicates that almost no low molecular weight component is present in this system. In other studies[24–26] results indicate that this secondary transition is associated with the relaxations of movements of polymer segments in the length of entangle-

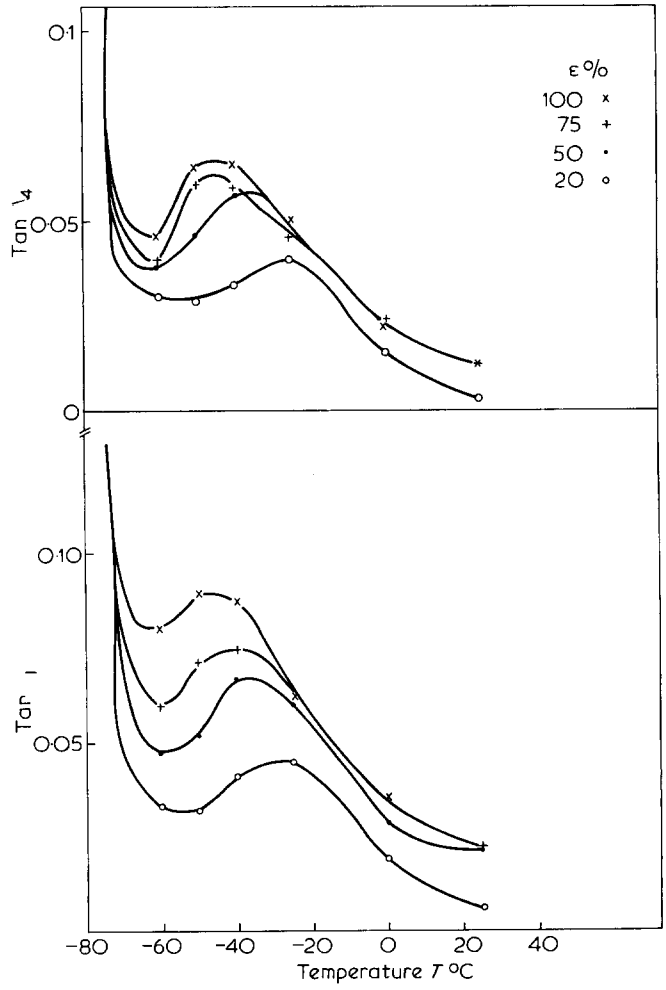

Figure 9 The loss function (tan Λ) obtained in the 1st and 4th cycles *versus* temperature and as a function of strain for B-3 composition (ϕ = 15%)

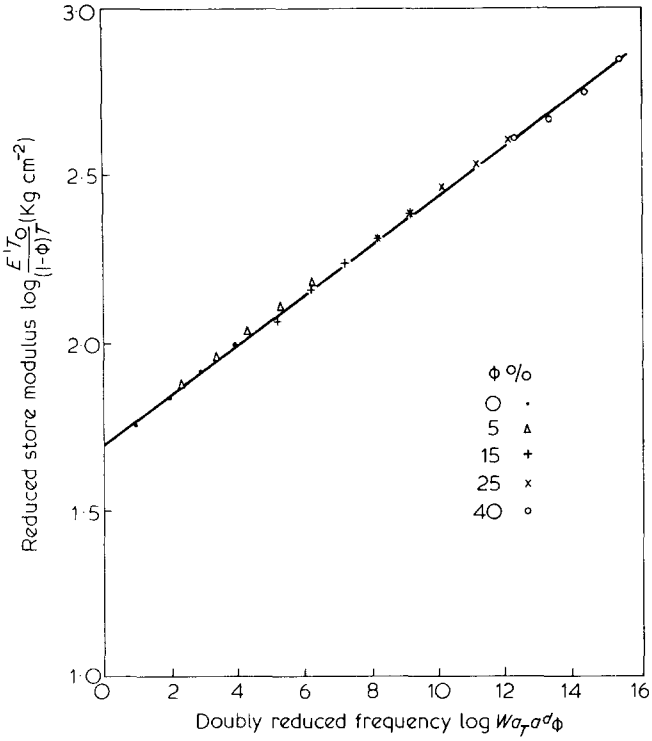

Figure 10 Storage modulus ***versus*** doubly reduced frequency

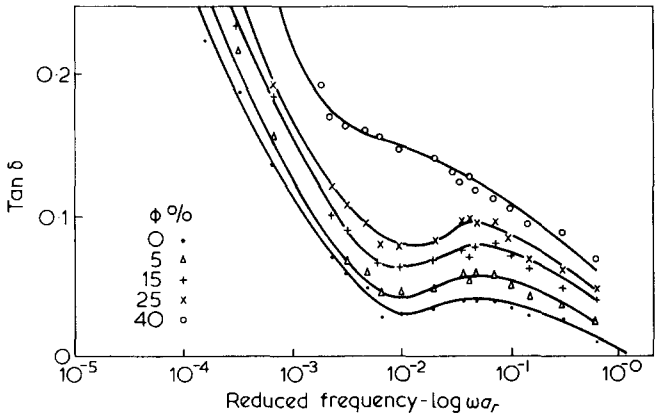

Figure 11 Tan δ versus reduced frequency as a function of filler content

ments, and it was also found that this transition is effected by the filler[27].

In additional studies[28], it was shown that for an uncrosslinked polymer in the glassy region, the effective surface energy connected with the failure of the polymer is a linear function of the average molecular weight M:

$$\gamma = \gamma_\infty - bM^{-1} \qquad (18)$$

where γ_∞ and b are experimental constants. It was found that when the average molecular weight equals the molecular weight between entanglements, the surface energy becomes equal to zero.

It can be assumed that in a filled crosslinked polymer where $M_c \geqslant M_e$, the surface energy will not become zero but will reach a certain minimum. Thus if the second transition is associated with the release of movements of polymer segments, and their length is equal to the distance between chemical or physical crosslink points, the interface energy between the filler and the binder will reach a minimum in this region and a higher degree of dewetting will occur. Therefore the higher the degree of dewetting the higher the maximum obtained for this secondary transition.

Attenuation of wave propagation

The storage modulus was calculated through equation (5) from the attenuation and wave velocity obtained when a sinusoidal wave was excited through a rod shape specimen of the material. Then using the shift factors $-\log a_T$ and $\log a^d_\phi$ [18], all the data was shifted to one master curve. *Figure 10* describes the reduced storage modulus ***versus*** the doubly reduced frequency. It can be seen that the same shift factors obtained from the static data could be used for the dynamic data, although the values of $E_1(\omega)$ were found to be a little higher than $E(t)$ at the corresponding time $-t = 1/\omega$, as also was observed elsewhere[29]. When the store modulus is compared to the modulus obtained when the wave was superimposed on a static strain of 20%, higher values were obtained which result from the softening effect[30].

From equations (5) and (17) tan δ was calculated and then shifted using the shift factor $-\log a_T$. The result for the materials investigated are illustrated in *Figure 11*. The results are similar to the results for the loss function tan Λ. Higher values for tan δ are obtained when the wave is superimposed on a static strain as it is illustrated in *Figure 12*. While for hysteresis, dewetting is directly measured, in the wave propagation experiment measurements are conducted after dewetting corresponding to the strain level applied has been completed. Therefore, higher damping with higher degree of dewetting is expected, as the main mechanisms responsible for the energy absorption are dependent on the degree of dewetting.

SUMMARY

Successive hysteresis experiments may be used for characterization of the main processes that are responsible for the increase in energy absorption when an unreinforced filler is added to an elastomer. The results indicate that the higher damping and softening effect observed in the system investigated are mainly due to dewetting. Friction between unbonded filler particles, rearrangement of torn molecule configurations and dewetting of rewetted attachements, play only a secondary role in the increase of the damping. It was shown that the softening energy given by equation (14) gives a quantitative measure of the dewetting energy.

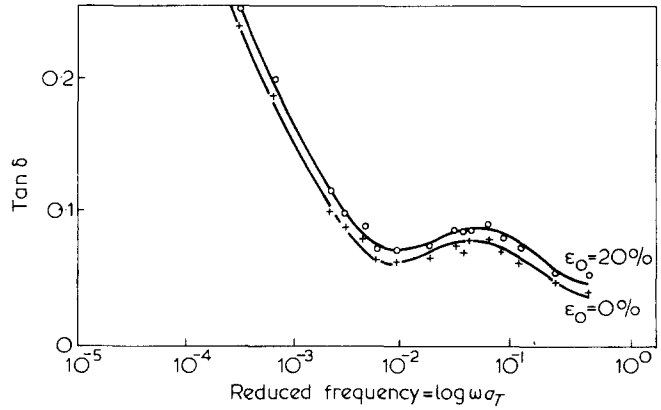

Figure 12 The influence of static strain on tan δ for B-3 composition (ϕ = 15%)

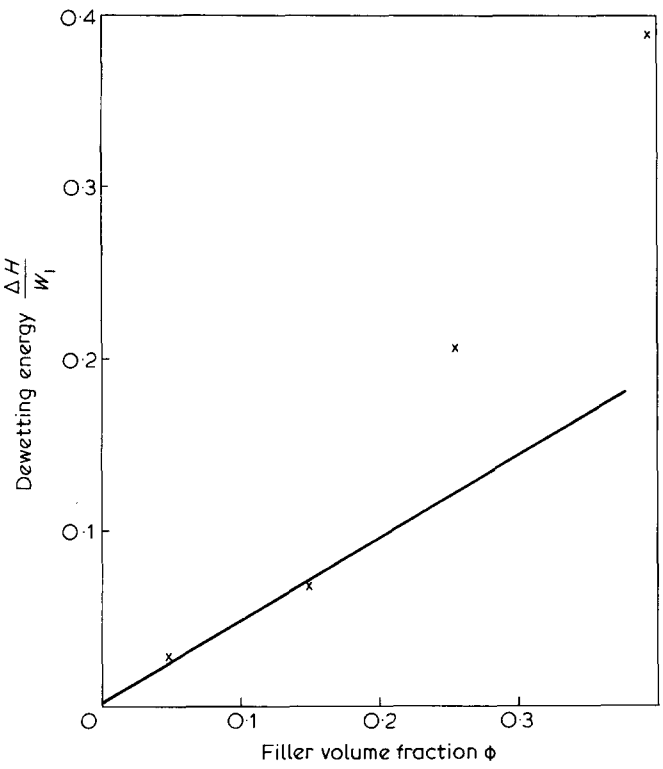

Figure 13 The softening energy *versus* the filler volume fraction

Definition of a loss function (tan Λ) indicates the existence of a transition above the glass transition. The transition intensity and temperature were dependent on the degree of dewetting, but could not be related directly to dewetting because this transition exists also in the pure polymer.

Higher filler volume fractions show higher damping. Higher ϕ increase the interface surface area:

$$S = \frac{6\phi}{d_f} \tag{19}$$

where d_f is the particle diameter. Therefore it is expected that the increase in dewetting energy will be linear with ϕ. On the other hand, the stress concentration existing on particles surfaces decreases the effective strength of the interface bonds and therefore increases the tendency to dewetting. It was shown[31] that the stress concentration is a function of the ratio d_i/d_f where d_i is the distance between two neighbour particles. This ratio is a function of $\phi^{1/3}$, therefore a deviation from linearity should be expected when dewetting energy is plotted against the filler volume fraction particularly at high filler content (as can be seen in *Figure 13*). Larger particles increase the tendency to dewetting, and higher dewetting energies were obtained when filler with larger particles was used.

Figures 8 and *9* indicate that while for the pure polymer the loss function is independent of the strain level, the filled compositions show such dependency in particular at the secondary transition region. This nonlinear behaviour results from the fact that every strain level represents a different material that is characterized by a different dewetting level. Similar results were obtained when a longitudinal wave was generated through the material. Higher filler content leads to the higher wave attenuation.

REFERENCES

1 Einstein, A. *Ann. Physic.* 1906, **19**, 289
2 Guth, E. *J. Appl. Phys.* 1945, **16**, 20
3 Van der Poel, C. *Rheol. Acta.* 1958, **1**, 198
4 Hashin, Z. *Appl. Mech. Rev.* 1964, **17**, 1
5 Laudel, R. F. *Mechanics and Chemistry of solid propellant* (Ed. Eringen, A. C. *et al. 4th Symp. on Naval Structural Mechanics* (April 1965) Pergamon Press, p 575
6 Waterman, H. A. *Rheol.Acta.* 1966, **5**, 140; *ibid* 1969, **8**, 22
7 Boehme, R. D. *J. Appl. Polym. Sci.* 1968, **12**, 1097
8 Waterman, P. C. and Truell, R. *J. Math. Phys.* 1961, **2**, 512
9 Everett, D. H. *Trans. Farad. Soc.* 1952, **48**, 949; *ibid* 1954, **50**, 187, 1077; *ibid* 1955, **51**, 1551
10 Harwood, J. A. C., Mullins, L. and Payne, A. R. *J. Appl. Polym. Sci.* 1965, **9**, 3011
11 Caruthers, J. M., Cohen, R. E. and Medalia, A. I. *Rubber Chem. Technol.* 1976, **49**, 1076
12 Blanchard, A. F. and Parkinson, D. *Ind. Eng. Chem.* 1952, **44**, 799
13 Harwood, J. A. C. and Payne, A. R. *J. Appl. Polym. Sci.* 1966, **10**, 315
14 Fedors, R. F. and Landel, R. F. *J. Polymer. Sci.* 1975, **13**, 579
15 Murphy, R. *The Role of filler elastomer adhesion in the reinforcement of SBR vulcanizates* Ph.D. Thesis submitted to the University of Akron, USA (1974)
16 Klosner, J. M., Segal, A. and Franklin, H. N. *J. Appl. Phys.* 1968, **39**, 15
17 Hillier, K. W. and Kolsky, H. *Proc. Phys. Soc.* 1949, **62**, 111
18 Diamant, Y. and Folman, M. *Polymer* 1979, **20**, 1025
19 Fowks, F. M. *ASTM* STP No. 360, 1960, p 20
20 Gil, M. *Crosslinking and characterization of polymers based on PBCT* M. Sc. thesis submitted to the Technion, Israel (1972)
21 Derman, D. *Nonlinear viscoelastic analysis of a thick sphere with finite strains*, Ph. D. thesis submitted to the Technion, Israel (1973)
22 Lepie, A. H. and Adicoff, A. *J. Appl. Polym. Sci.* 1972, **16**, 1155
23 Sidorovich, E. A. *et al. Rubber Chem. Tech.* 1971, **44**, 166; *Polymer Sci.* 1974, USSR **16(4)**, 993
24 Boyer, R. F. *Preprint of papers presented at the 175th Meeting of the ACS, Div. of Org. Coat. and Plast. Chem.* Anaheim, USA, May 12–17, 1978, **38**, P-379, 387
25 Gillham, I. K. and Boyer, R. F. Reference 24, p 366
26 Ferry, J. D. et al. *J. Phys. Chem.* 1964, **68**, 3414
27 Gillham, J. K. *private communciations*
28 Moon, P. C. and Barker, R. E. *J. Polym. Sci.* 1973, **11**, 909
29 Tobolsky, A. V. *Properties and structure of polymers* Wiley, USA, 1960
30 Payne, A. R. and Whittaker, R. E. *J. Appl. Polym. Sci.* 1972, **16**, 1191
31 Adams, D. F., Douer, D. R. and Thomas, R. L. *Mechanical behaviour of fiber-reinforced composite materials* AFML-TR-67-96, p 72